

Research progresses in 3D-MRI on ankle cartilage injuries

WANG Qian, WU Yanbo, PAN Shinong, ZHANG Guangxin*

(Department of Radiology, Shengjing Hospital of China Medical University, Shenyang 110004, China)

[Abstract] Ankle joint cartilage injuries could lead to severe pain and limited joint activity, and early diagnosis of ankle joint cartilage injury is particularly important. 3D-MR sequences has good diagnostic efficiency for ankle joint cartilage injuries. The research progresses of 3D-MRI in diagnosing ankle cartilage injuries were reviewed in this article.

[Keywords] ankle joint; cartilage; magnetic resonance imaging

DOI: 10.13929/j.issn.1003-3289.2024.05.033

踝关节软骨损伤 3D-MRI 研究进展

王倩, 吴艳波, 潘诗农, 张光昕*

(中国医科大学附属盛京医院放射科, 辽宁 沈阳 110004)

[摘要] 踝关节软骨损伤易致剧烈疼痛而使关节活动受限, 早期诊断非常重要。3D-MRI 用于诊断踝关节软骨损伤具有较好效能。本文针对 3D-MRI 诊断踝关节软骨损伤研究进展进行综述。

[关键词] 踝关节; 软骨; 磁共振成像

[中图分类号] R684; R445.2 **[文献标识码]** A **[文章编号]** 1003-3289(2024)05-0791-04

踝关节又称为距小腿关节, 由胫、腓骨下端及距骨滑车组成, 是人体主要承重关节之一, 活动度较大, 与直立和行走紧密相关^[1]。退行性骨关节炎和急性损伤是造成踝关节损伤的两大常见原因, 早期前者表现为软骨变性, 后者则表现为软骨、韧带和肌腱损伤^[2]。相对于有创的“金标准”关节镜检查, MRI 是目前临床较常用于诊断软骨损伤的影像学方法, 不仅能清晰显示关节内结构, 还具有无辐射、无创等优势。近年出现的包括 3D-MRI 技术、超短回波时间序列^[3]、定量 MR T1、T2 及 T1 ρ 成像^[4]、延迟钆增强软骨 MRI^[5]、化学交换饱和转移成像^[6]等新兴关节软骨成像技术用于诊断关节软骨损伤具有较大潜在价值。本文就 3D-MRI 诊断踝关节软骨损伤研究进展进行综述。

1 关节软骨生理及病理基础

关节软骨指附着于关节端的透明软骨, 不仅使粗糙不平的关节面变得光滑, 还能减少运动时关节面之

间的摩擦、缓冲震荡和冲击^[7]。关节软骨由软骨细胞与其周围的细胞外基质共同构成, 可分为表浅层、过渡层、辐射层及钙化层。细胞外基质的主要成分为蛋白聚糖、II 型胶原纤维及水^[8], 蛋白聚糖和胶原纤维等共同维持软骨渗透压, 对保持软骨机械功能具有重要作用。II 型胶原纤维在辐射层中呈垂直分布, 在过渡层呈“拱门样”分布, 于表浅层则呈平行分布; 其中的辐射层蛋白聚糖含量最多、水含量最低, 故 T2 弛豫时间较短而呈低信号, 表浅层蛋白聚糖含量逐渐减少、水含量逐渐增加, 使其 T2 弛豫时间变长、信号逐渐增加^[9]。见图 1。

踝关节软骨损伤可致关节剧烈疼痛及活动受限^[10-11], 相关病理改变包括蛋白聚糖含量减少、II 型胶原纤维断裂及软骨渗透压降低, 影像学表现为 T2 弛豫时间延长、T2WI 表现为较高信号。因关节软骨缺乏血管、神经和淋巴等组织^[8], 自我修复能力差,

[第一作者] 王倩(1999—), 女, 山西晋城人, 在读硕士。研究方向: 骨骼肌肉系统影像学。E-mail: wq20593198@126.com

[通信作者] 张光昕, 中国医科大学附属盛京医院放射科, 110004。E-mail: gx.z@163.com

[收稿日期] 2024-01-30 [修回日期] 2024-03-25

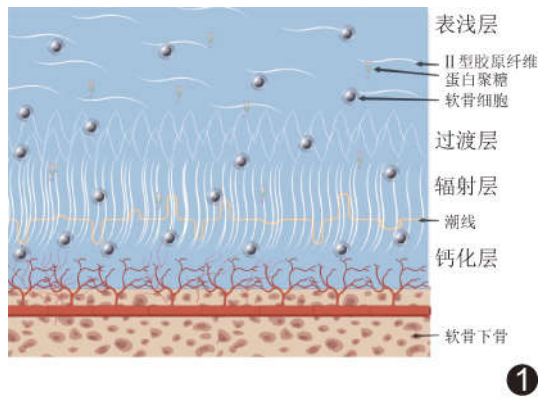


图 1 关节软骨的结构示意图

再生能力低^[12], 损伤后较难治愈, 故早期诊断关节软骨损伤是改善预后的关键。

2 3D-MRI 用于踝关节软骨成像的优势

目前用于踝关节 MR 检查的常规序列包括 2D 质子密度加权成像、T2W 及 T1W, 其优点是能较好地显示踝关节解剖结构; 但因踝关节软骨相对菲薄^[13], 导致图像对比度一般且空间分辨力不足, 区分关节软骨、关节腔积液及软骨下骨等时可遭遇困难^[14]; 或受限于磁场均匀性, 脂肪抑制不均匀而妨碍显示软骨损伤信号。相比 2D 序列, 3D-MR 序列具有明显优势^[15], 通常仅需采集矢状位图像, 通过多角度重建获取其他方位图像, 不仅有助于提高检查效率^[16-17], 还能通过不同角度观察踝关节解剖结构及软骨形态; 且 3D 序列扫描层厚相对较薄, 空间分辨力高, 能减少空间层面的相互干扰, 明显提升关节软骨与邻近骨质及关节积液间的对比度, 更为准确、灵敏地显示踝关节软骨损伤^[18]。

3 3D-MRI 诊断踝关节软骨损伤

3.1 三维稳态采集快速成像 (three-dimensional fast imaging employing steady-state acquisition, 3D-FIESTA)

作为稳态自由进动梯度回波技术的一种^[19], 3D-FIESTA 在回波采集后施加一个与空间编码梯度场大小相同而方向相反的梯度场, 使所有方向上的相位得到重聚, 并且采集自由衰减 (free induction delay, FID) 信号、自旋回波 (spin echo, SE) 信号和受激回波 (stimulated echo, STE) 信号的融合信号而达到真正的稳态^[20], 使其图像质量和信噪比 (signal-to-noise ratio, SNR) 均优于常规梯度回波序列, 可显示较为细小的解剖结构。一项关于膝关节软骨损伤的 MRI 研究^[21]结果表明, 经关节镜验证, 3D-FIESTA 序列诊断软骨损伤的准确率为 90% 以上。另外, 由于

3D-FIESTA 序列信号强度与组织的 T2/T1 比值相关^[22], 该序列图像中组织的 T2/T1 比值越大则信号越高^[23], 如关节液、脂肪及血液^[24], 而 T2/T1 比值较小的肌肉、韧带及软骨等则表现为较低信号。因此, 3D-FIESTA 序列图像中软骨与周围组织的对比度较高, 可较为灵敏地显示表浅软骨损伤。另外, 高信号的脂肪也能与软骨形成较好的对比, 关节液较少时也能较好地显示关节软骨。3D-FIESTA 的不足主要表现为对于磁场均匀性较为敏感, 易产生条纹状伪影而干扰显示病变。

3.2 3D-CUBE

3D-CUBE 属三维快速自旋回波序列, 以较长回波链采集结合半傅里叶采集及自动校正并行成像和重建; 回波时间长导致磁化转移效应降低, 软骨信号强度和 3D 图像的 SNR 增高; 另一方面, 回波时间较长引起的 T2 衰减也使得图像的模糊效应较 2D 图像更为明显^[25]。既往研究^[26]发现, 3D-CUBE 序列对于显示踝关节软骨、韧带等细微结构较常规 2D 序列具有明显优势; 后续研究^[16]通过引入新的加速技术——CAIPIRINHA 而进一步缩短扫描时间, 且使图像空间分辨率及对比度均得到大幅提升。3D-CUBE 可通过一次采集多个回波得到无间隔连续薄层图像, 在一定程度上减少部分容积效应、提高软骨和关节腔积液的 SNR 及软骨和软骨下骨的对比度噪声比^[27], 其中, 软骨表现为中等信号, 关节腔积液则为较高信号^[28], 二者构成良好对比度, 故能较为清晰地显示软骨损伤。此外, 利用该序列还能全面显示踝关节韧带的起止点、走行及形态等, 可直接据以判断韧带损伤程度。

3.3 三维双回波稳态 (three-dimensional dual-echo steady-state, 3D-DESS)

3D-DESS 序列为水激发 3D 薄层序列, 能够较好地兼顾扫描时间与成像质量, 是较为敏感的 MR 软骨成像序列, 用于显示关节软骨具有明显优势^[29], 其诊断软骨损伤的敏感度和准确率甚至高于有创的关节镜检查^[30-31]。本质上 3D-DESS 序列是稳态进动快速成像 (fast imaging with steady-state precession, FISP) 与反转 FISP (reserved FISP, PSIF) 的结合^[32], 即在 1 个 TR 内同时采集 FID 和 SE 信号, 利用平方和算法将重建后的 2 种信号叠加, 以获得 SNR 较高的 3D-DESS 图像。3D-DESS 图像中, 关节腔积液呈高信号^[33]、骨和脂肪为较低信号, 踝关节软骨则表现为中-高信号; PSIF 产生的重 T2 效果可突出显示液体的 T2WI 较高信号, 有助于更好地区别关节腔积液与关节软骨。此外, 亦有研究^[34-35]表明 3D-

DESS 序列可用于半自动分割软骨和神经成像。

3.4 三维扰相脂肪抑制梯度回波(three-dimensional fat-suppressed spoiled gradient-recalled, 3D-FS-SPGR) 3D-FS-SPGR 序列是在梯度回波采集 FID 信号后,于层面选择梯度方向上增加一个“扰相梯度”,以破坏 SE 信号和 STE 信号,使残留的质子横向磁矩在下次射频脉冲之前达到完全去相位,为目前公认的显示软骨形态的优质序列^[36],能较 2D-T2 脂肪饱和序列更为准确地提示软骨损伤^[37]。该序列的特点是采用较短的 TR 和 TE,且其 FA 较小,扰相梯度可减少对 T2 的影响,故具有 T1 加权性质^[38],可抑制关节腔液体信号而使其呈现为低信号,叠加脂肪抑制作用可增强踝关节软骨信号,使踝关节软骨呈现为相对高信号^[39];而脂肪抑制可使软骨下骨信号降低、增加关节软骨与软骨下骨的对比度,显示踝关节软骨更为清晰。利用 3D-FS-SPGR 能准确显示踝关节软骨的厚度、是否存在裂隙,以及损伤程度和范围,有利于临床诊断和治疗。但该序列属暗液序列,软骨与关节腔积液对比度较差,故诊断关节软骨表浅性损伤的敏感度较差,且成像时间较长、较易产生运动伪影亦为其局限性。

4 小结与展望

踝关节解剖结构较为复杂。相比关节镜及 2D-MR 序列,3D-MR 序列能以多角度、于多方位无创清晰显示踝关节软骨形态,对早期检出踝关节软骨损伤极为重要,具有较高临床应用潜力。另一方面,3D-MRI 技术也存在一些缺点,如成像时间长、患者难以配合,图像运动伪影较重等,期待未来逐步加以改进。

利益冲突:全体作者声明无利益冲突。

作者贡献:王倩查阅文献、撰写文章;吴艳波查阅文献、修改文章;潘诗农、张光昕指导、审阅文章。

[参考文献]

- [1] FONG D T, HONG Y, CHAN L K, et al. A systematic review on ankle injury and ankle sprain in sports[J]. *Sports Med*, 2007, 37(1):73-94.
- [2] DING C, CICUTTINI F, SCOTT F, et al. Sex differences in knee cartilage volume in adults: Role of body and bone size, age and physical activity[J]. *Rheumatology (Oxford)*, 2003, 42(11): 1317-1323.
- [3] CHANG E Y, DU J, CHUNG C B. UTE imaging in the musculoskeletal system[J]. *J Magn Reson Imaging*, 2015, 41(4): 870-883.
- [4] ECK B L, YANG M, ELIAS J J, et al. Quantitative MRI for evaluation of musculoskeletal disease: Cartilage and muscle composition, joint inflammation, and biomechanics in osteoarthritis[J]. *Invest Radiol*, 2023, 58(1):60-75.
- [5] ZILKENS C, TIDERIUS C J, KRAUSPE R, et al. Current knowledge and importance of dGEMRIC techniques in diagnosis of hip joint diseases[J]. *Skeletal Radiol*, 2015, 44(8):1073-1083.
- [6] WATKINS L E, RUBIN E B, MAZZOLI V, et al. Rapid volumetric gagCEST imaging of knee articular cartilage at 3 T: Evaluation of improved dynamic range and an osteoarthritic population[J]. *NMR Biomed*, 2020, 33(8):e4310.
- [7] SCHÜTZ U H, BILLICH C, SCHOSS D, et al. MRI cartilage assessment of the subtalar and midtarsal joints during a transcontinental ultramarathon: New insights into human locomotion[J]. *Int J Sports Med*, 2018, 39(1):37-49.
- [8] ARMIENTO A R, STODDART M J, ALINI M, et al. Biomaterials for articular cartilage tissue engineering: Learning from biology[J]. *Acta Biomater*, 2018, 65:1-20.
- [9] ZIBETTI M V W, MENON R G, de MOURA H L, et al. Updates on compositional MRI mapping of the cartilage: Emerging techniques and applications [J]. *J Magn Reson Imaging*, 2023, 58(1):44-60.
- [10] 韩宇,常非,姜振德,等.距骨软骨损伤:病因、诊断、治疗及前景[J]. *中国组织工程研究*, 2019, 23(15):2443-2449.
- [11] 高丽香,袁慧书. T1 ρ 技术定量评估踝关节距骨软骨损伤[J]. *中国医学影像技术*, 2020, 36(3):444-447.
- [12] WU J, CHEN Q, DENG C, et al. Exquisite design of injectable hydrogels in cartilage repair[J]. *Theranostics*, 2020, 10(21): 9843-9864.
- [13] 罗慕晴,李宏伟,向辉春,等. 3.0T MR T1 ρ 及 T2mapping 评估兔股骨内侧踝关节软骨退变[J]. *中国医学影像技术*, 2022, 38(10):1446-1451.
- [14] XU Y, HE L, HAN Y, et al. Evaluation of 3-dimensional magnetic resonance imaging (3D MRI) in diagnosing anterior talofibular ligament injury[J]. *Med Sci Monit*, 2021, 27:e927920.
- [15] BAILLIE P, COOK J, FERRAR K, et al. Magnetic resonance imaging findings associated with posterior ankle impingement syndrome are prevalent in elite ballet dancers and athletes[J]. *Skeletal Radiol*, 2021, 50(12):2423-2431.
- [16] FRITZ B, BENSLER S, THAWAIT G K, et al. CAIPIRINHA-accelerated 10-min 3D TSE MRI of the ankle for the diagnosis of painful ankle conditions: Performance evaluation in 70 patients[J]. *Eur Radiol*, 2019, 29(2):609-619.
- [17] FRITZ B, FRITZ J, SUTTER R. 3D MRI of the ankle: A concise state-of-the-art review[J]. *Semin Musculoskelet Radiol*, 2021, 25(3):514-526.
- [18] YAN W, MENG X, SUN J, et al. Intelligent localization and quantitative evaluation of anterior talofibular ligament injury using magnetic resonance imaging of ankle [J]. *BMC Med Imaging*, 2021, 21(1):130.
- [19] TOUSKA P, CONNOR S E J. Recent advances in MRI of the head and neck, skull base and cranial nerves: New and evolving sequences, analyses and clinical applications [J]. *Br J Radiol*,

- 2019, 92(1104):20190513.
- [20] SUN Q, DONG M J, TAO X F, et al. Dynamic MR imaging of temporomandibular joint: An initial assessment with fast imaging employing steady-state acquisition sequence[J]. *Magn Reson Imaging*, 2015, 33(3):270-275.
- [21] LI X, YU C, WU H, et al. Prospective comparison of 3D FIESTA versus fat-suppressed 3D SPGR MRI in evaluating knee cartilage lesions[J]. *Clin Radiol*, 2009, 64(10):1000-1008.
- [22] LI B, HUANG Y, ZHANG Y, et al. Utilizing pre-operative MR imaging and adapting optimal needle puncture approach to improve radiofrequency ablation fraction of thoracic dorsal root ganglia[J]. *Sci Rep*, 2021, 11(1):18589.
- [23] ZHANG Y, HE X, LI J, et al. An MRI study of the tibial nerve in the ankle canal and its branches: A method of multiplanar reformation with 3D-FIESTA-C sequences[J]. *BMC Med Imaging*, 2021, 21(1):51.
- [24] ZHANG J, HAO D, DUAN F, et al. The rotating stretched curved planar reconstruction of 3D-FIESTA MR imaging for evaluating the anterior cruciate ligament of the knee joint[J]. *Magn Reson Imaging*, 2019, 55:46-51.
- [25] BAJAJ S, CHHABRA A, TANEJA A K. 3D isotropic MRI of ankle: Review of literature with comparison to 2D MRI [J]. *Skeletal Radiol*, 2024, 53(5):825-846.
- [26] NOTOHAMIPRODJO M, KUSCHEL B, HORNG A, et al. 3D-MRI of the ankle with optimized 3D-SPACE [J]. *Invest Radiol*, 2012, 47(4):231-239.
- [27] YI J, LEE Y H, HAHN S, et al. Fast isotropic volumetric magnetic resonance imaging of the ankle: Acceleration of the three-dimensional fast spin echo sequence using compressed sensing combined with parallel imaging[J]. *Eur J Radiol*, 2019, 112:52-58.
- [28] CHEN C A, KIJOWSKI R, SHAPIRO L M, et al. Cartilage morphology at 3.0T: Assessment of three-dimensional magnetic resonance imaging techniques[J]. *J Magn Reson Imaging*, 2010, 32(1):173-183.
- [29] 朱乐发, 肖叶玉, 夏学文, 等. 不同翻转角双回波稳态序列 MRI 评价膝关节骨性关节炎软骨损伤[J]. *中国医学影像技术*, 2020, 36(11):1697-1701.
- [30] SCHLEICH C, HESPER T, HOSALKAR H S, et al. 3D double-echo steady-state sequence assessment of hip joint cartilage and labrum at 3 Tesla: Comparative analysis of magnetic resonance imaging and intraoperative data [J]. *Eur Radiol*, 2017, 27(10):4360-4371.
- [31] KOHL S, MEIER S, AHMAD S S, et al. Accuracy of cartilage-specific 3-Tesla 3D-DESS magnetic resonance imaging in the diagnosis of chondral lesions: Comparison with knee arthroscopy[J]. *J Orthop Surg Res*, 2015, 10:191.
- [32] STAROSWIECKI E, GRANLUND K L, ALLEY M T, et al. Simultaneous estimation of T₂ and apparent diffusion coefficient in human articular cartilage in vivo with a modified three-dimensional double echo steady state (DESS) sequence at 3 T [J]. *Magn Reson Med*, 2012, 67(4):1086-1096.
- [33] KWON D, LEE C, CHAE Y, et al. Clinical validation of the 3-dimensional double-echo steady-state with water excitation sequence of MR neurography for preoperative facial and lingual nerve identification [J]. *Imaging Sci Dent*, 2022, 52 (3): 259-266.
- [34] JEONG H S, KIM Y, KIM H J, et al. Imaging of facial nerve with 3D-DESS-WE-MRI before parotidectomy: Impact on surgical outcomes[J]. *Korean J Radiol*, 2023, 24(9):860-870.
- [35] BACH CUADRA M, FAVRE J, OMOUMI P. Quantification in musculoskeletal imaging using computational analysis and machine learning: Segmentation and radiomics [J]. *Semin Musculoskelet Radiol*, 2020, 24(1):50-64.
- [36] von ENGELHARDT L V, KRAFT C N, PENNEKAMP P H, et al. The evaluation of articular cartilage lesions of the knee with a 3-Tesla magnet [J]. *Arthroscopy*, 2007, 23(5):496-502.
- [37] HAN C H, PARK H J, LEE S Y, et al. IDEAL 3D spoiled gradient echo of the articular cartilage of the knee on 3.0 T MRI: A comparison with conventional 3.0 T fast spin-echo T2 fat saturation image [J]. *Acta Radiol*, 2015, 56(12):1479-1486.
- [38] XIA Y, ZHENG S. Reversed laminar appearance of articular cartilage by T1-weighting in 3D fat-suppressed spoiled gradient recalled echo (SPGR) imaging [J]. *J Magn Reson Imaging*, 2010, 32(3):733-737.
- [39] DU M, JIANG L, WANG A, et al. MR imaging provides practical information for preoperative assessment of radial polydactyly with bifurcation at the metacarpophalangeal joint level [J]. *Int J Gen Med*, 2022, 15:2163-2169.